CHAPTER IV

RESULTS AND DISCUSSION

4.1 Control Experiments

This part aimed to determine the *o*-toluidine removal from each individual constituent of fluidized-bed Fenton process as specified in Table 3.1 in Chapter 3. The initial conditions used in these experiments were as follows: 1 mM of *o*-toluidine, 1 mM of Fe^{2+}, 17 mM of H_2O_2, pH 3 and 100 g of carriers. The results are shown in Figure 4.1. If both Fenton's reagents (Fe^{2+} and H_2O_2) were not presented in the solution, the removal of *o*-toluidine was only 4.7 % in 120 minutes. For the control experiments without H_2O_2 and without Fe^{2+}, the *o*-toluidine removals were 3.4% and 8.8% in 120 minutes, respectively. More than 90% of Fe^{2+} and H_2O_2 still present in the solution at the end of the experiment. Due to its vapor pressure of 0.2 kPa, volatilization of *o*-toluidine to the atmosphere could be a minor leak. Therefore, it is implied that the major depletion of *o*-toluidine was from the adsorption to the carriers (SiO_2) and apparatus. From all these results, it is proved that *o*-toluidine could not be removed effectively without an involvement of hydroxyl radicals from Fenton's reaction under the studied condition.

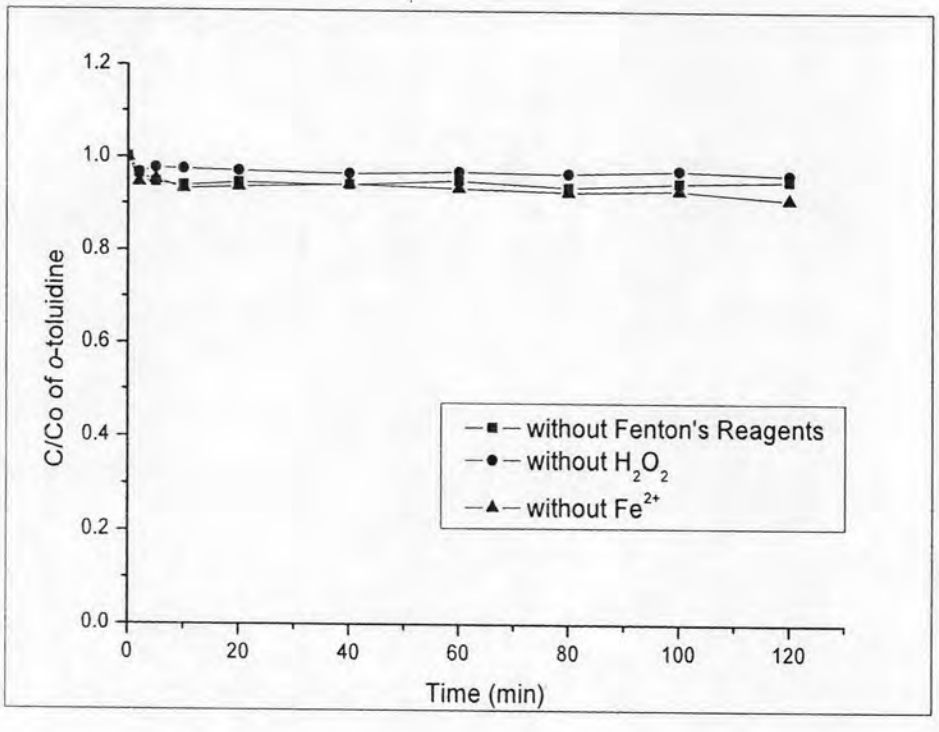

Figure 4.1 Control experiments for fluidized-bed reactor

4.2 Screening Tests by Two-level Factorial Design

Major factors that possibly affected the performance of the fluidized-bed Fenton process were pH, initial Fe^{2+} and H_2O_2 concentrations, and the amount of carriers. These four factors were selected as the inputs into the two-level factorial design. The highest and lowest levels of each factor were specified the program. Table 3.2 in Chapter 3 summarizes the factors and their levels tested in the two-level factorial design study. With those 2 levels of 4 factors, the total number of experiment runs was 16 (= 2^4). The responses were *o*-toluidine, COD, and total iron removal efficiencies.

Table 4.1 shows the experimental results from the two-level factorial design. The "-1" and "+1" signs for each variable represented the low and the high levels, respectively. The removal of *o*-toluidine from the two-level factorial design experiments were between 6.7% and 64.2%, the COD removal were between 0% and 36.7%, and the total iron removal were between 1.9% and 100%.

In order to effectively screen the significant factors from those insignificant ones, a half-normal plot, the effects versus their assigned half-normal probability, was drawn (Zhang et al., 2009) as shown in Figure 4.2. The significant factors were selected from the factors that fell off the straight line, which were initial Fe^{2+} concentration (B) and initial H_2O_2 concentration (C). These two factors also gave higher correlations with *o*-toluidine removal (0.868 and 0.364). While the pH (A) and the amount of carriers (D) were closer to the line and gave lower correlation number (0.015 and 0.113). The significant factors selected were also the same as obtained from the ANOVA test shown in Table 4.2.

Table 4.1 Results of the experiments from two-level factorial design

Run number	pH	Fe^{2+} (mM)	H_2O_2 (mM)	Carriers (g)	*O*-toluidine removal (%)	COD removal (%)	Total iron removal (%)
1	−1	−1	−1	−1	6.7	0	23.1
2	−1	−1	−1	+1	22.4	0	27.4
3	+1	−1	−1	−1	14.9	0	100
4	+1	−1	−1	+1	16.2	0	100
5	−1	+1	−1	−1	34.8	8.8	3.3
6	−1	+1	−1	+1	34.4	20.4	2.5
7	+1	+1	−1	−1	37.6	11.7	25.6
8	+1	+1	−1	+1	43.9	18.8	59.8
9	−1	−1	+1	−1	19.1	4	13.5
10	−1	−1	+1	+1	19.9	7.8	20.9
11	+1	−1	+1	−1	21.2	6	100
12	+1	−1	+1	+1	16.6	5.6	100
13	−1	+1	+1	−1	60.5	36.7	1.9
14	−1	+1	+1	+1	64.2	36.7	2.7
15	+1	+1	+1	−1	52.8	20.5	28.1
16	+1	+1	+1	+1	63.1	25.4	49.9

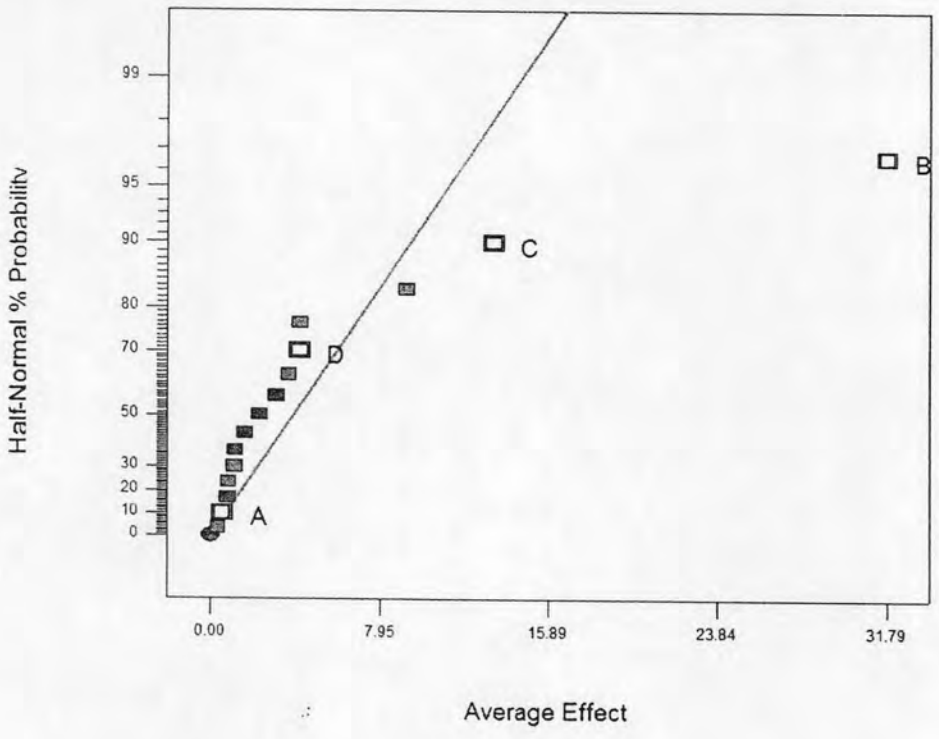

Figure 4.2 Half-normal % probability versus average effect

Table 4.2 ANOVA test for the response function of *o*-toluidine removal in two-level factorial design

Source	Sum of Squares	df	Mean Squares	F value	p-value Prob > F
Model	4820.30	4	1205.08	24.57	< 0.0001
A (pH)	1.16	1	1.16	0.024	0.8808
B (Fe^{2+})	4041.78	1	4041.78	82.41	< 0.0001
C (H_2O_2)	708.89	1	708.89	14.45	0.0029
D (Carriers)	68.48	1	68.48	1.40	0.2623
Residual	539.52	11	49.05		
Total (corr)	5359.82	15			

The Model F-value of 24.57 and p-value less than 0.05 implied that the model performed in this design was significant. Fe^{2+} (B) and H_2O_2 (C) also have the p-value less than 0.05 (<0.0001 and 0.0029, respectively). The average effects of the significant factors are shown in Figure 4.3a-b. The figure shows the effect of increasing factor's concentration, from the lowest to the highest level, on o-toluidine removal while the other factors were fixed at center level.

Both initial Fe^{2+} and H_2O_2 concentrations showed positive effect, which means the removal of *o*-toluidine increased as the level of these factors increased. From Figure 4.3a, the *o*-toluidine removal increased from 17.1% to 48.9% when the initial Fe^{2+} increased from 0.1 mM to 1 mM. While the increase in initial H_2O_2 concentration in from 1 mM to 17 mM could increase the *o*-toluidine removal from 26.4% to 39.7%. This was due to both Fe^{2+} and H_2O_2 were the Fenton's reagent. Fe^{2+} reacted with H_2O_2 to generate ·OH, which had powerful ability to degrade organic pollutants such as *o*-toluidine (Wang, 2008; Titus et al., 2004). Therefore, increasing initial Fe^{2+} and H_2O_2 concentrations could directly increase *o*-toluidine degradation.

For the insignificant factors, their average effects can be seen in Figure 4.4. The amount of carriers showed slightly positive effect on the removal of *o*-toluidine. The *o*-toluidine removal increased only 31% to 35.1% when the carriers increased from 50 g to 100 g. However, the carriers seemed to have more positive effect on the removal of total iron because the carriers in fluidized-bed Fenton process primarily served as solids particulates where iron could crystallize onto their surface. The effects on total iron removal can be seen in the data from Table 4.1. When other conditions are the same, most experiments conducted with the higher amount of carriers have higher total iron removals. Iron oxide coated on the carriers can re-dissolved via reductive dissolution and/or heterogeneous reaction to become Fe^{2+}, so the removal of *o*-toluidine can increase. However, this insignificant factor was excluded from further experiments for determining the optimum conditions for the removal of *o*-toluidine; hence, it was kept constant at 100 g.

Figure 4.4 (b) shows that there is no difference in *o*-toluidine removal when increasing pH from 2 to 4 (32.8% to 33.8%, respectively.) Although pH was also an insignificant factor, it could not be excluded from optimization study. This was due to the non-linearity of the effect of pH within this range (2-4), and as stated earlier, the Fenton process has the highest efficiency when pH is around 3 (Neyens and Baeyens, 2003). The effect of pH will be discussed further in section 4.2.2.

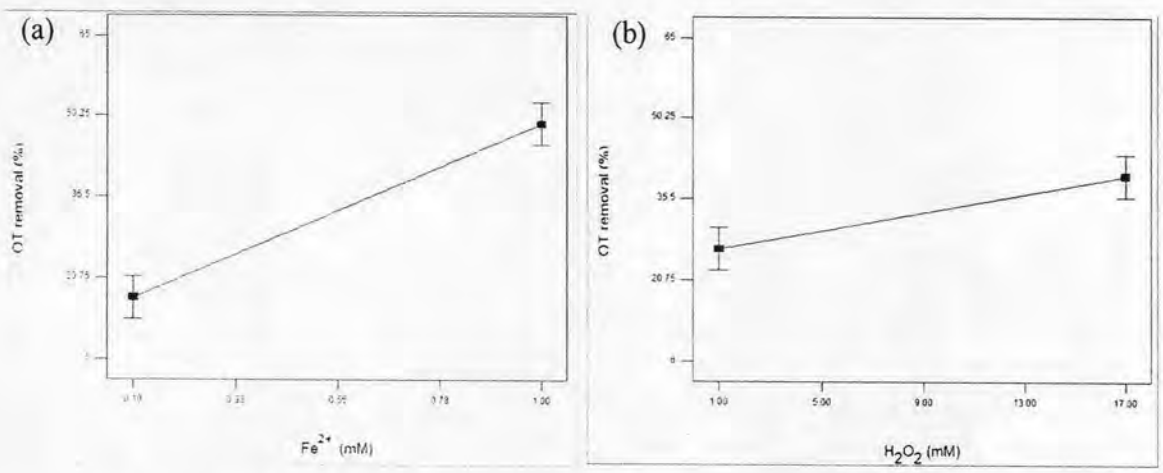

Figure 4.3 Average effects of significant factors on *o*-toluidine removal

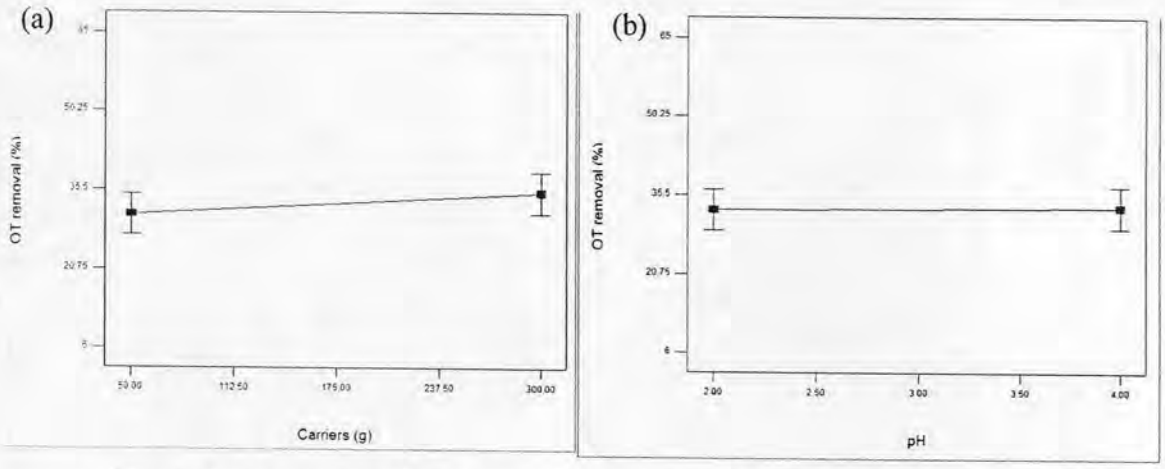

Figure 4.4 Average effects of insignificant factors on *o*-toluidine removal

4.3 Optimization by the Box-Behnken Design

The Box-Behnken experiment design was used to investigate the effect of the three variables obtained from previous parts and to determine the optimum conditions (Box and Behnkin, 1960), which maximizing the removals of *o*-toluidine and COD. Table 3.4 in Chapter 3 shows the levels of the three factors used in the design, i.e., pH (A), initial Fe^{2+} (B) and H_2O_2 (C) concentrations. The low, center, and high levels of each factor were designated as "–1", "0", and "+1", respectively. The number of runs from Box-Behnken design was 17, which consisted of 5 repeating runs of the center levels. The responses were also the same as in the case of the two-level factorial design, i.e., *o*-toluidine, COD, and total iron removals.

The results from the experiments are shown in Table 4.3. The removal of *o*-toluidine from Box-Behnken design experiments were between 12.8% and 99.8%. Most *o*-toluidine removal resulted from Box-Behnken design were higher than those obtained from two-level factorial design. This is because of the effect of pH, which is shown in Figure 4.5. At pH 3, the *o*-toluidine removal was higher than the removal obtained from pH 2 and 4. It can also be seen from Table 4.3 that the highest removal of *o*-toluidine (99.8%) was obtained at pH 3 (Run #12 in Table 4.3) as compared to the experiments conducted at same Fe^{2+} and H_2O_2 but different pH (Run #13-#16 in Table 4.1). The similar trend was also obtained by many studies working with Fenton reaction (Dutta et al., 2002; Kuo, 1992; Neyens and Baeyens, 2003). When pH is higher or lower than 3, the *o*-toluidine removal efficiency became lower. This was due to the high amount of free Fe^{2+} at low pH such as 2, which had lower activity than $Fe(OH)^+$ at pH 3-4, and the formation of $Fe(OH)_3$ that had low activity at higher pH (Wang, 2008; Malik and Saha, 2003).

Figure 4.6 shows the response surface plot of two effects on *o*-toluidine removal efficiency. From the plot, Y-axis is *o*-toluidine removal (%) and other two are the two key factors. It can be seen that all plots were convex shape. Each point on the surface represents the *o*-toluidine removal at each value of factors.

Figure 4.6 (a) shows the response surface plot of the effect of initial Fe^{2+} and H_2O_2 concentrations on *o*-toluidine removal efficiency at pH 3. Both factors also showed the positive effect similar to those obtained from the two-level factorial design. It can be seen that when initial Fe^{2+} concentration was at low level (0.1 mM), increasing initial H_2O_2 concentration from 1 to 17 mM could not increase the

Table 4.3 Results of the experiments from Box-Behnken design

Run Number	pH	Fe^{2+} (mM)	H_2O_2 (mM)	*O*-toluidine removal (%)	COD removal (%)	Total iron removal (%)
1	−1	−1	0	12.8	4.1	7.7
2	+1	−1	0	17.1	3.1	91.1
3	−1	+1	0	49.9	19.4	5.2
4	+1	+1	0	52.2	14.7	29.5
5	−1	0	−1	29.7	16.7	4.3
6	+1	0	−1	34.2	17.4	48.3
7	−1	0	+1	41.5	22.1	5.4
8	+1	0	+1	39.1	32.4	41
9	0	−1	−1	18.9	0	10.2
10	0	+1	−1	56	17	24.7
11	0	−1	+1	15.2	5.2	8.8
12	0	+1	+1	99.8	61.8	18
13	0	0	0	71.4	25.8	39.1
14	0	0	0	71.8	25	39
15	0	0	0	72.4	24.8	40.9
16	0	0	0	71.5	26.1	37
17	0	0	0	72.6	24.4	40.2

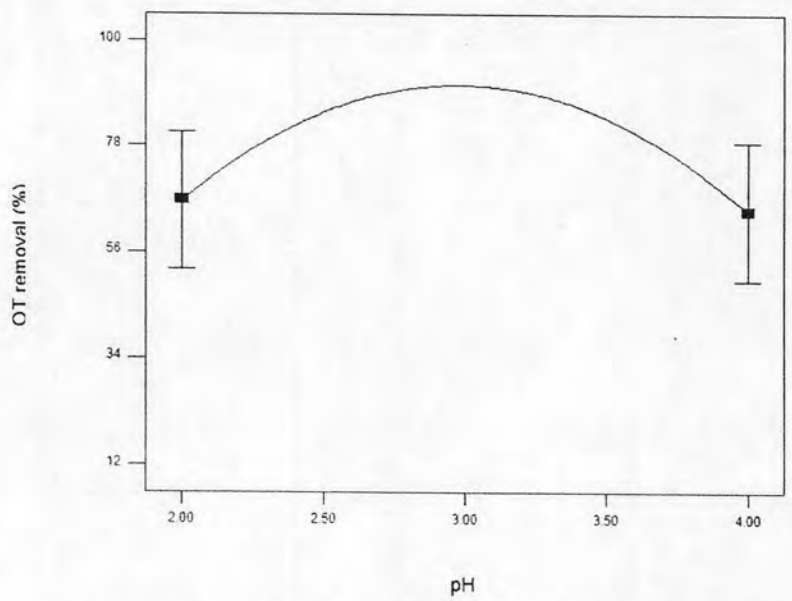

Figure 4.5 Effect of pH on *o*-toluidine removal

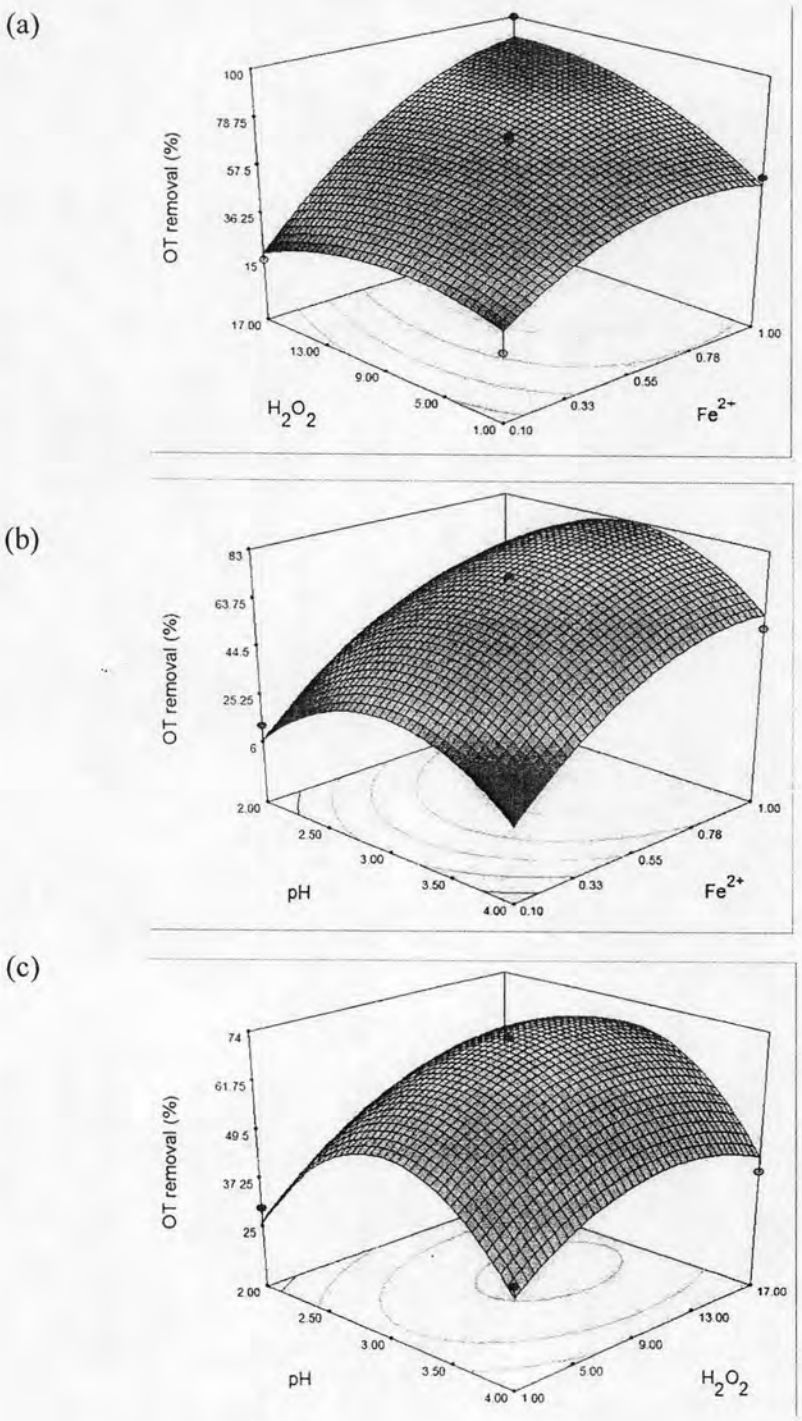

Figure 4.6 Response surface plots of the effects on *o*-toluidine removal efficiency

o-toluidine removal efficiency. This is because the amount of Fe^{2+} was not enough to react with H_2O_2 and too high H_2O_2 could cause a scavenging effect on the hydroxyl radicals and sequentially deteriorated the removal efficiency (Kang et al., 2002). In contrast, when initial Fe^{2+} concentration increased to higher level (0.55 and 1 mM), increasing initial H_2O_2 concentration from 1 to 17 mM could significantly increase the removal efficiency.

The condition for the removal of *o*-toluidine by fluidized-bed Fenton process can be optimized by the quadratic polynomial equation obtained from the Box-Behnken design. Two equations were established to explain the mathematic relationship between o-toluidine removal and the significant variables (the equation in terms of coded factors and actual factors):

$$\text{o-toluidine removal} = 71.94 + 1.09A + 24.24B + 7.10C - 0.50AB - 1.73AC + 11.88BC - 25.14A^2 - 13.80B^2 - 10.67C^2 \quad (4.1)$$

where, A, B and C are pH, initial Fe^{2+} and H_2O_2 concentrations, respectively.

$$\text{o-toluidine removal} = -220.39 + 153.01pH + 105.61[Fe^{2+}] + 2.90[H_2O_2] - 1.11pH[Fe^{2+}] - 0.22pH[H_2O_2] + 3.16[Fe^{2+}][H_2O_2] - 24.90pH^2 - 69.36[Fe^{2+}]^2 - 0.17[H_2O_2]^2 \quad (4.2)$$

Both equations were used to calculate the *o*-toluidine removal at each value of pH, Fe^{2+} and H_2O_2 concentrations. Equation (4.1) used the level of each factor to calculate (coded factors: –1, 0 or +1), while equation (4.2) used the real value of each factor (actual factors.) By this way, the optimum condition can be determined. Firstly, the value of all factors must be selected. The maximum level was selected in case of *o*-toluidine and COD removals because they are the required results from the experiments. The other factors such as pH were selected to be in the range used in this study. Next, the software provided the runs of experiments that give maximum removal with various levels of each factor. Then one suitable condition was selected to conduct the experiment to verify the accuracy of the model.

Finally, the highest *o*-toluidine removal efficiency was predicted to be 90.2% (COD removal efficiency of 41.4%) at the optimal pH, initial Fe^{2+} and H_2O_2 concentrations of 3, 1 mM and 17 mM, respectively. The optimum condition for the removal of *o*-toluidine (1 mM concentration) by fluidized-bed Fenton process as predicted by the model was shown in Table 4.4. It can be seen that the optimum conditions were similar to Run #12 in Table 4.3; however, the *o*-toluidine and COD removals were lower than those from real experiment.

Table 4.4 Predicted o-toluidine, COD, and total iron removals by Fluidized-bed Fenton process at the optimum conditions for 1 mM of *o*-toluidine and 100 g of carriers.

	Experimental Variables			Responses		
	pH	Fe^{2+} (mM)	H_2O_2 (mM)	*O*-toluidine removal (%)	COD removal (%)	Total iron removal (%)
Predicted Value	3	1	17	90.2	41.4	22.1

The analysis of variance (ANOVA) test was conducted and presented in Table 4.5. It indicates that the predictability of the model was at 95% confidence level. The model predictions were in good correlation with the experimental data ($R^2 = 0.9605$). The Model F-value of 18.89 and the values of "Prob > F" less than 0.05 implied the model was significant. The "Lack of Fit F-value" of 479.99 implied the Lack of Fit was significant. There is only a 0.01% chance that a "Lack of Fit F-value" this large could occur due to noise. Most statistical tests of errors, the residuals were interpreted as errors, assuming they followed a normal distribution.

Figure 4.7 shows a plot of normal % probability versus residuals. A plot that was nearly linear suggested normal distribution of the residuals. A plot that obviously departed from linearity suggested that the error distribution was not normal, which could be seen as the error from 5 repeated runs (Runs #13 - #17 in Table 4.3).

Figure 4.8 represents the plot between actual and predicted value of *o*-toluidine removal from the model. Each point in the figure represents the result of *o*-toluidine removal from experiments. It can be seen that most actual values from experiments (X axis) are higher than from prediction (Y axis). So, it is usual when using the prediction from the model and found the higher removal in actual experiment, as in the optimum condition in this study.

Figure 4.9 shows the results from the optimum condition. From Figure 4.9 (a), *o*-toluidine was degraded rapidly in the first minute, after that the reaction rate was slow down but continued to degrade 99.8% in 120 minutes. COD was also decreased with time, but with lower rate as shown in Figure 4.9 (b), and the total COD removal in 120 minutes is less than that of *o*-toluidine. This was due to many organic intermediates produced from the reaction. For the Fenton's reagents, both Fe^{2+} and H_2O_2 decreased with time because they were used for the reaction of generating ·OH (equation 2.5). In the beginning, there were plenty of Fenton's reagents, so the reaction could happen very fast as shown by the *o*-toluidine degradation. After that, the Fenton-like reaction happened. This was the reaction between H_2O_2 and Fe^{3+}. It can be seen in Figure 4.9 (c) and (d) that after most of Fe^{2+} was used, H_2O_2 still decreased.

Table 4.5 ANOVA test for response function of *o*-toluidine removal in Box-Behnken design

Source	Sum of Squares	df	Mean Square	F value	p-value Prob > F
Model	10099.23	9	1122.14	18.89	0.0004
A (pH)	9.46	1	9.46	0.16	0.7017
B (Fe^{2+})	4797.10	1	4797.10	80.75	< 0.0001
C (H_2O_2)	432.18	1	432.18	7.27	0.0308
AB	1.00	1	1.00	0.017	0.9004
AC	11.90	1	11.90	0.20	0.6680
BC	517.56	1	517.56	8.71	0.0214
A^2	2609.52	1	2609.52	43.93	0.0003
B^2	830.58	1	830.58	13.98	0.0073
C^2	502.09	1	502.09	8.45	0.0228
Residual	415.86	7	59.41		
Lack of Fit	414.71	3	138.24	479.99	< 0.0001
Pure Error	1.15	4	0.29		
Total (corr)	10515.09	16			

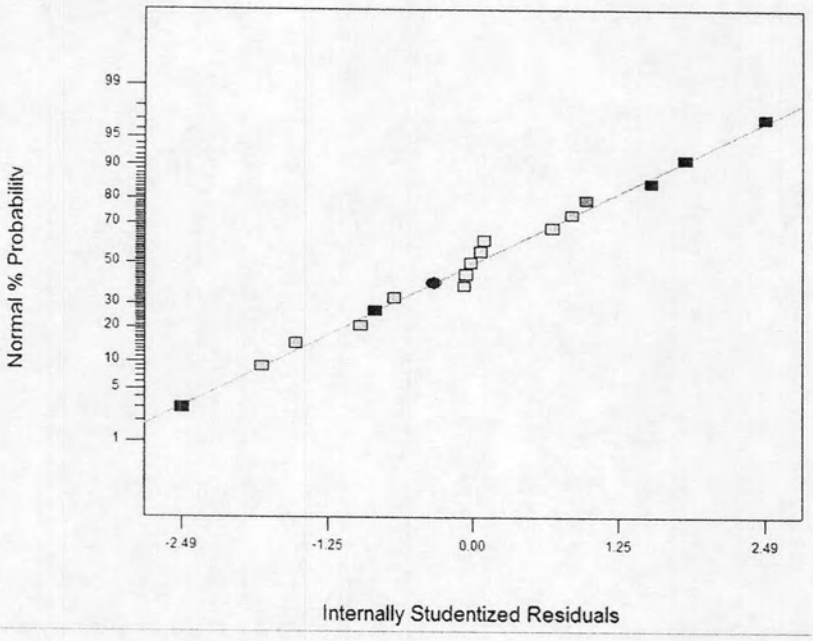

Figure 4.7 Normal plot of residuals

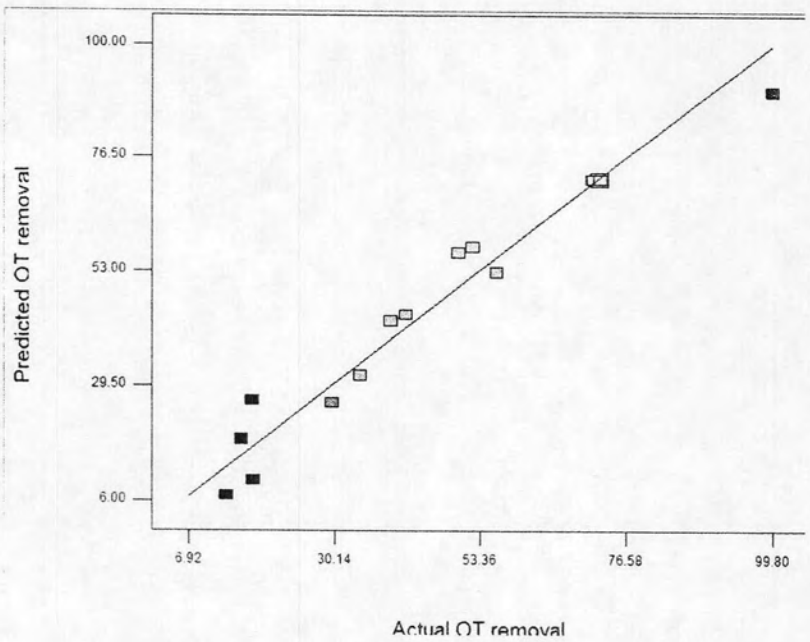

Figure 4.8 Actual versus predicted value of *o*-toluidine removal

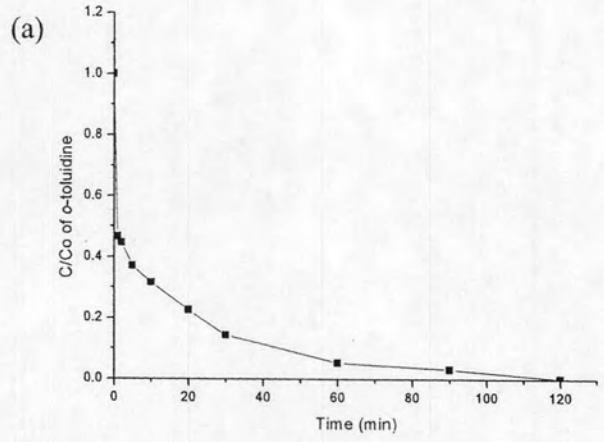

O-toluidine removal

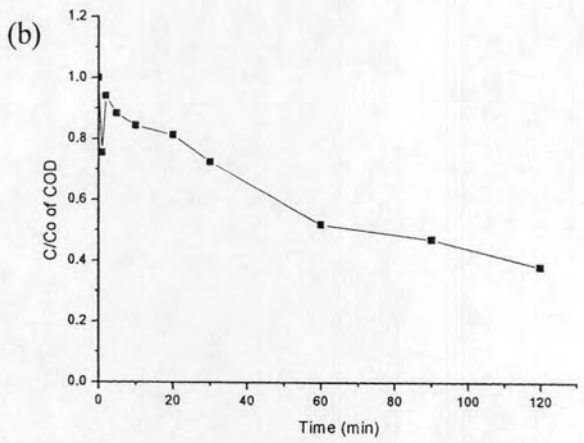

COD removal

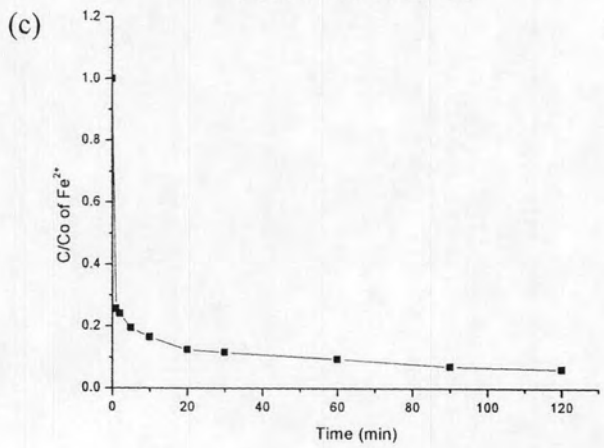

Fe^{2+} remaining

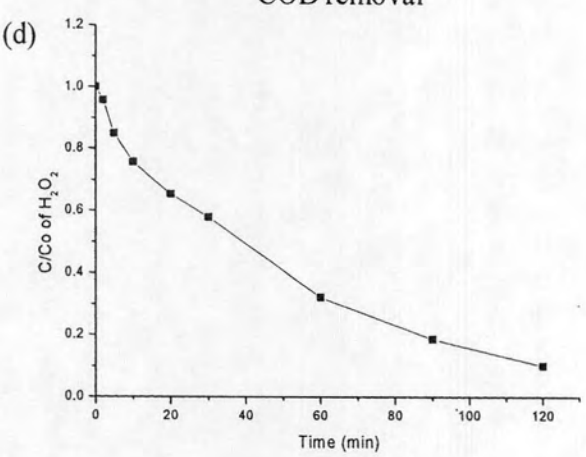

H_2O_2 remaining

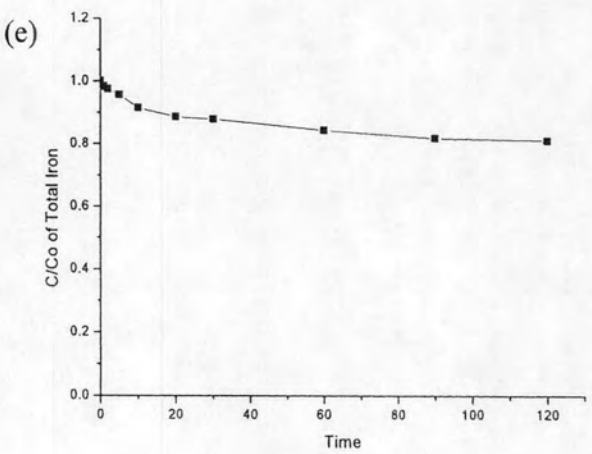

Total iron removal

Figure 4.9 Results from the optimum condition

Moreover, *o*-toludine degradation still happened but with slow rate, it conformed to the slow rate of Fenton-like reaction (Safarzadeh-Amiri et al., 1996). For the advantage of fluidized-bed Fenton process, Fe^{3+} generated can be removed by crystallization with SiO_2. Figure 4.9 (e) shows the total iron removal at the optimum condition, where 18.8% of total iron was removed within 120 minutes. The removal of total iron can result in the decrease of $Fe(OH)_3$ sludge, which can happen when adjusting pH back to normal after treatment. However, low total iron removal at this condition was due to the pH used in the optimum condition, which was 3. It was lower than pH used for removing iron, which should be 3.5 – 4 (Diz and Novak, 1998).

4.4 Kinetic Study

In this part, the kinetics of *o*-toluidine oxidation by hydroxyl radicals in the fluidized-bed Fenton process was investigated. Three independent variables were studied including *o*-toluidine, Fe^{2+}, and H_2O_2 concentrations.

4.4.1 Two Stages Reaction

Results from the experiment showed that the oxidation rate of *o*-toluidine gradually slowed down after 1 minute. From Figure 4.10 (a), it can be seen that it is a two-stage reaction. The oxidation rate of *o*-toluidine before 1 minute was more rapid than that after 1 minute.

The main reason for the two-stage reaction is that Fe^{2+} reacts with H_2O_2 very quickly (equation 2.5 in Chapter 2). Therefore, the produced ·OH could react with *o*-toluidine quickly in the first stage. This stage is referred as the Fe^{2+}/H_2O_2 stage. After Fe^{2+} reacts with H_2O_2, it will become Fe^{3+}. Fe^{3+} can also react with H_2O_2 to produce $\cdot HO_2$ (hydroperoxyl radicals) and Fe^{2+} (equation 2.9 and 2.10 in Chapter 2). This Fe^{2+} regeneration can produce more ·OH to degrade *o*-toluidine. However, ·OH is slowly produced in this step because the reaction rate constant of Fe^{3+} reacting with H_2O_2 (0.01 $M^{-1}s^{-1}$) is less than that of Fe^{2+} reacting with H_2O_2 (76 $M^{-1}s^{-1}$) (Rivas et al., 2001; Walling and Goosen, 1973). Therefore, it could be understood that the degradation of *o*-toluidine in the second stage was from Fe^{3+} reacting with H_2O_2. That is the reason for slowly degradation of *o*-toluidine in this stage. The second stage is referred as Fe^{3+}/H_2O_2 stage (Lu et al., 1999).

The detection of Fe^{2+} also supports the theory of the two-stage reaction. As shown in Figure 4.10 (b), a change in Fe^{2+} was similar to that of *o*-toluidine degradation. Fe^{2+} decreased rapidly in 1 minute as it was transformed to Fe^{3+}.

In order to determine the kinetic information, the first and second stages must be discussed separately. The first stage reaction was determined by the initial rate, and the second stage was determined by the first-order rate.

4.4.2 Effect of *O*-toluidine Concentration on *O*-toluidine Oxidation

To determine the effect of *o*-toluidine on the oxidation rate, various *o*-toluidine concentrations of 0.5, 1, 2 and 5 mM were used with 1 mM of Fe^{2+}, 17 mM of H_2O_2, pH 3 and 100 g of SiO_2. The results are shown in Figure 4.10. From Figure 4.10 (a), it can be seen that only 0.5 and 1 mM of *o*-toluidine could be oxidized as highly as 100% within 120 minutes. Higher *o*-toluidine concentration resulted in lower oxidation rate in both stage of reactions and lower removal of *o*-toluidine. *O*-toluidine could be removed 49.1% when the concentration increased to 5 mM. In the Fe^{3+}/H_2O_2 stage, when *o*-toluidine concentration was up to 2 and 5 mM, the pseudo-first-order rate constants were very slow compared with those from 0.5 and 1 mM of

o-toluidine concentration. This was due to the intermediate products generated by *o*-toluidine oxidation, which could be the scavengers for ·OH. So, higher *o*-toluidine concentration means higher intermediate products that can compete with *o*-toluidine for ·OH consumption. For the total iron, *o*-toluidine concentrations in this range had not much effect on its removal, as shown in Figure 4.10 (d). The total iron removals were less than 20% for all experiments with different *o*-toluidine concentrations.

4.4.3 Effect of Fe^{2+} on *o*-toluidine oxidation

Fe^{2+} played an important role in catalyzing H_2O_2 to produce ·OH in Fenton reaction (Collins et al., 1959). Because the added amount of Fe^{2+} directly influenced the generation of ·OH (equation 2.5), it has a large impact on *o*-toluidine degradation. With these conditions: 1 mM of *o*-toluidine, 17 mM of H_2O_2, pH 3 and 100 g of SiO_2, effect of Fe^{2+} on the *o*-toluidine degradation was investigated by varying the concentration of Fe^{2+} to 0.1, 0.5, 1 and 2 mM, respectively.

The results are shown in Figure 4.11. The *o*-toluidine removal was proportional to the amount of Fe^{2+} added. *O*-toluidine removal efficiency of 15.5% with 0.1 mM Fe^{2+} could increase to 100% when Fe^{2+} increased to 2 mM, as shown in Figure 4.11 (a). In the Fe^{2+}/H_2O_2 stage, there was a large change in *o*-toluidine oxidation rate when higher amount of Fe^{2+} was added. For the Fe^{3+}/H_2O_2 stage, the same tendency was obtained. The rate constants are summarized in Table 4.7.

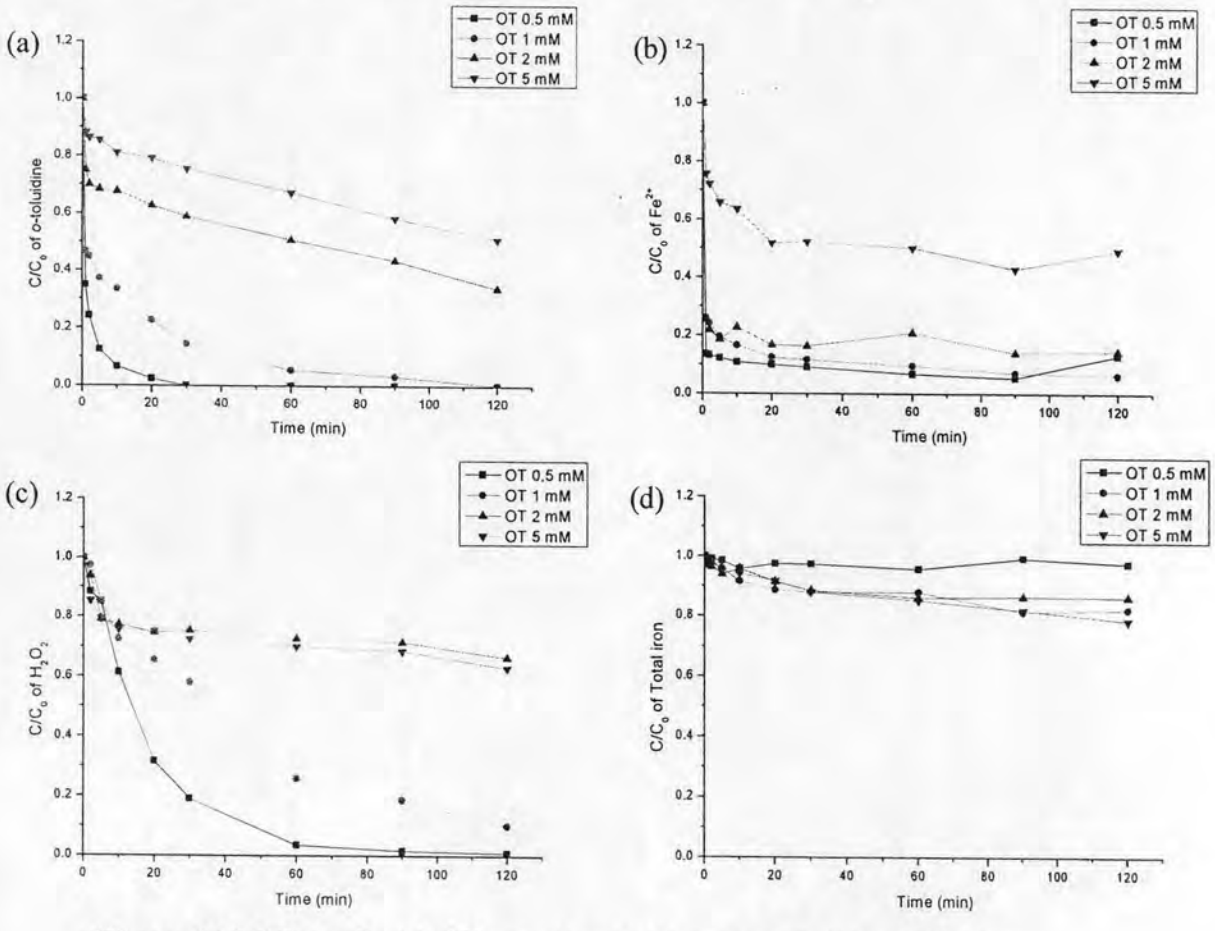

Figure 4.10 Effect of *o*-toluidine concentration on *o*-toluidine oxidation; *o*-toluidine concentration: 0.5, 1, 2 and 5 mM with parameter conditions; 1 mM of Fe^{2+}, 17 mM of H_2O_2, pH 3 and 100 g of SiO_2

Table 4.6 *O*-toluidine oxidation rates and rate constants at different initial concentrations.

o-toluidine concentration (mM)	Initial rate ($\times 10^{-4}$M min^{-1})	k ($\times 10^{-3}$min^{-1})
0.5	3.37	137
1	5.1	40
2	4.68	6
5	5.84	4

When Fe^{2+} was at low level, less ·OH was generated, which is the reason for low *o*-toluidine removal. In addition, high amount of H_2O_2 could promote a scavenging effect (equation 2.8) (Christensen et al., 1982). It can be seen from Figure 4.11 (b) and (c) that only about 10% of H_2O_2 was used when Fe^{2+} was 0.1 or 0.5 mM, so the ·OH generated was less than those generated from Fe^{2+} of 1 and 2 mM, which nearly 100% of H_2O_2 was used. On the other hand, higher Fe^{2+} could also have a scavenging effect on ·OH by equation 2.6 with the rate constant of 3.8×10^8 $M^{-1}s^{-1}$ (Stuglik and Zagorski, 1981). For the total iron, higher removal was obtained when Fe^{2+} concentration increased from 0.1 to 0.5 mM, this was due to more Fe^{3+} generated from the reaction that can crystallize onto the surface of SiO_2. However, for Fe^{2+} concentration up to 1 and 2 mM, the total iron removal could not increase further.

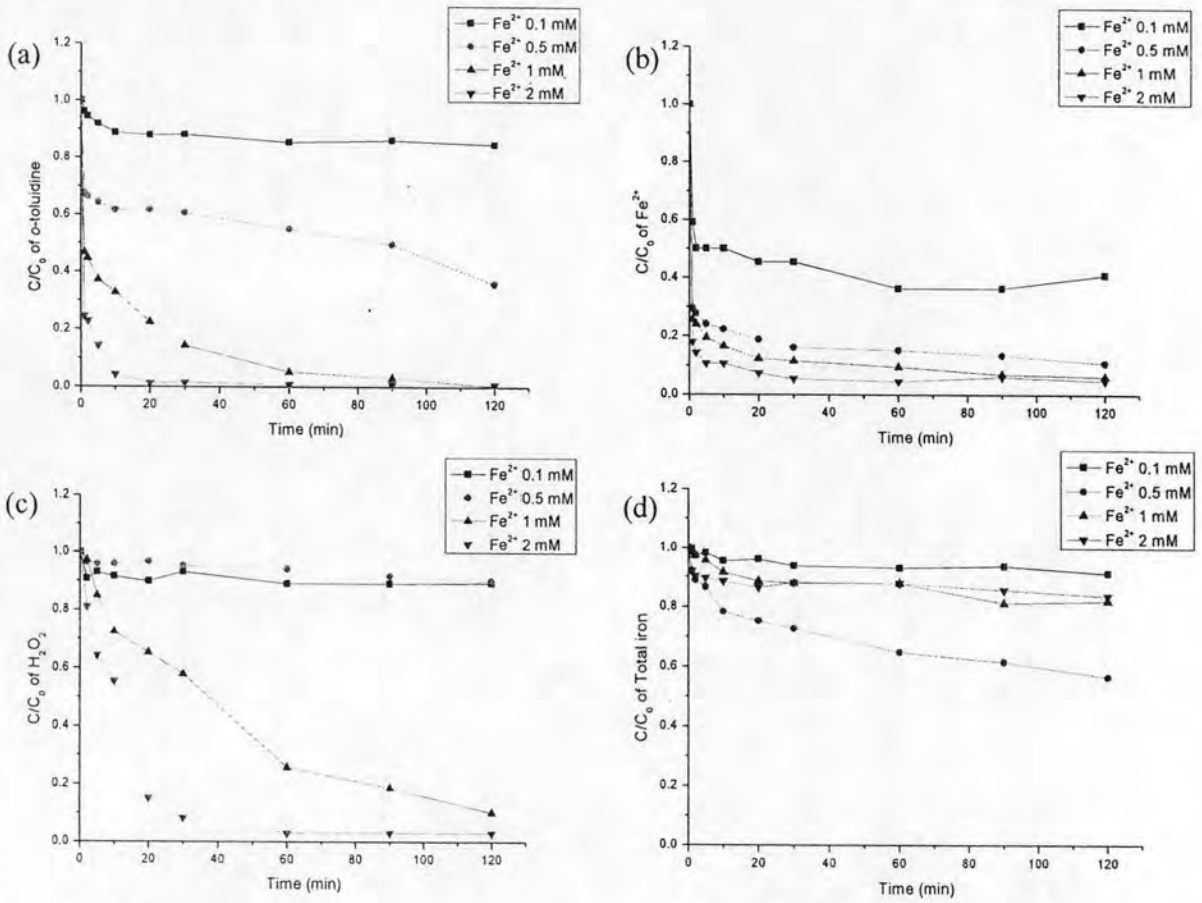

Figure 4.11 Effect of Fe^{2+} concentration on *o*-toluidine oxidation; Fe^{2+} concentration: 0.1, 0.5, 1 and 2 mM with parameter conditions; 1 mM of *o*-toluidine, 17 mM of H_2O_2, pH 3 and 100 g of SiO_2

Table 4.7 *O*-toluidine oxidation rates and rate constants at different initial Fe^{2+} concentration

Fe^{2+} concentration (mM)	Initial rate ($\times 10^{-4}$M min^{-1})	k_f ($\times 10^{-3} min^{-1}$)
0.1	0.4	0.8
0.5	3.24	4.4
1	5.1	40.3
2	7.44	157.5

This might be from the limit for crystallization onto the SiO_2 under this experimental condition. Therefore, the amount of Fe^{2+} used must be considered not only for *o*-toluidine removal but also total iron removal because less total iron removal means the higher $Fe(OH)_3$ sludge problem.

The pseudo-first-order rate constant (k_f) linearized with respect to Fe^{2+} as shown in Figure 4.12. With the equation from the figure, the relationship of k_f and Fe^{2+} can be expressed as follows:

$$k_f = 7120.98[Fe^{2+}]^{1.77} \quad (4.3)$$

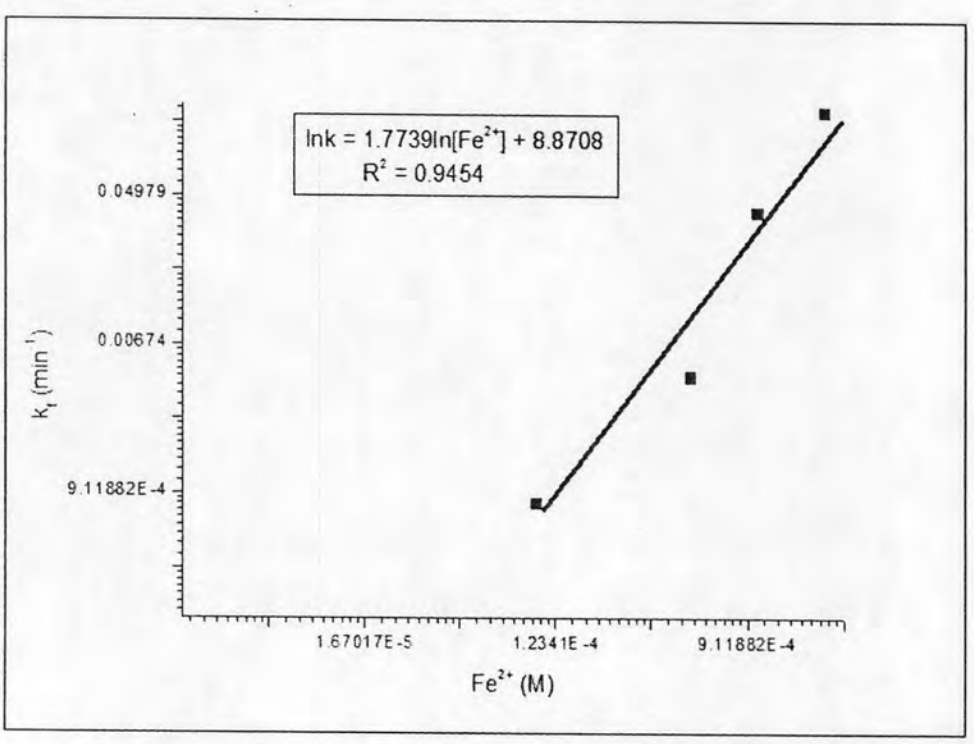

Figure 4.12 Relationship between pseudo-first-order rate constant and initial Fe^{2+} concentration; initial condition were as follows: 1 mM of *o*-toluidine, 17 mM of H_2O_2, pH 3 and 100 g of SiO_2

4.4.4 Effect of H_2O_2 on *o*-toluidine oxidation

H_2O_2 plays a part of oxidizing agent in the Fenton reaction. It was found in the control experiments that if only Fe^{2+} was added without H_2O_2, *o*-toluidine could not be degraded. In this section, various H_2O_2 concentrations of 1, 9, 17 and 34 mM were used to observe the effect of H_2O_2 on *o*-toluidine oxidation.The results are shown in Figure 4.13 and Table 4.8. The removal of *o*-toluidine increased from 66% to 100% when H_2O_2 concentration increased from 1 to 34 mM. The oxidation rate also increased with higher H_2O_2 concentration.

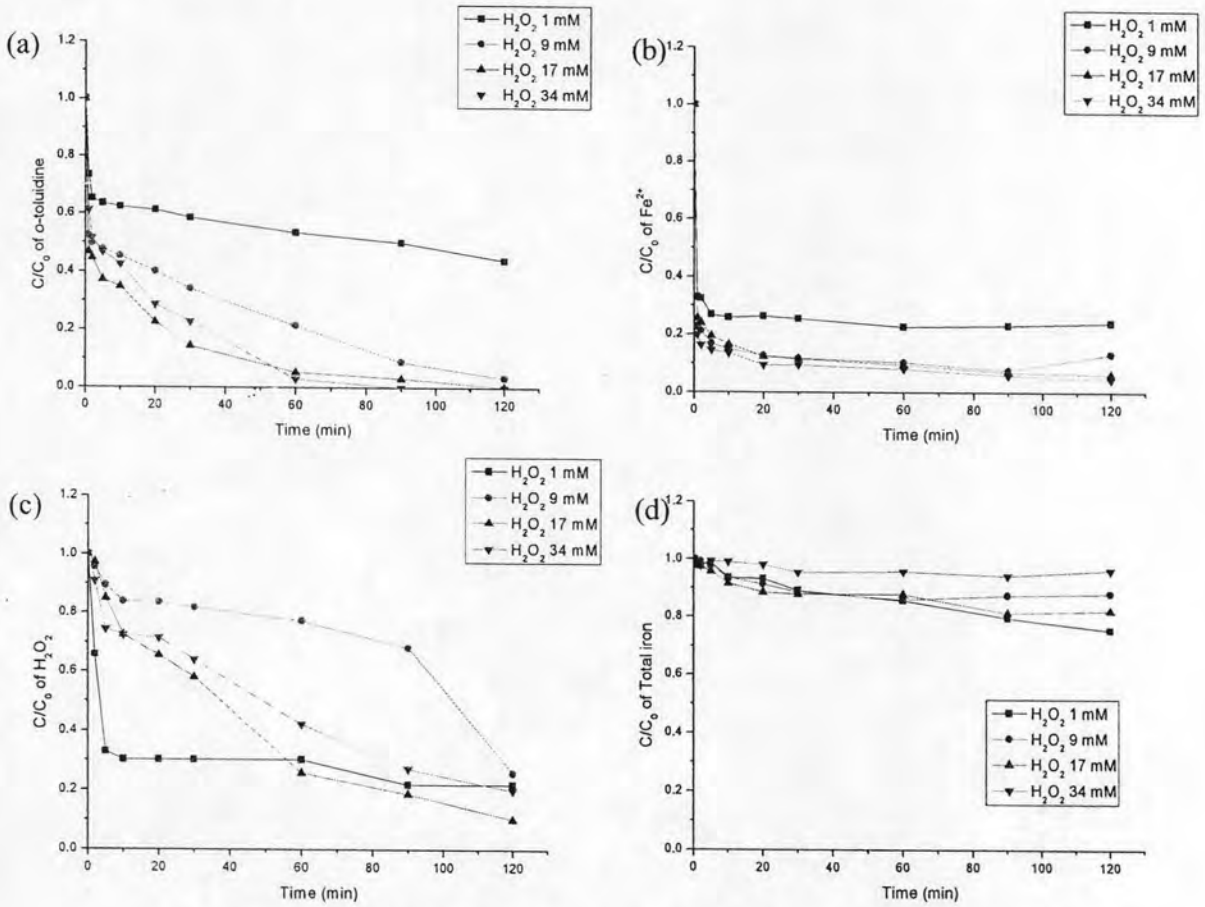

Figure 4.13 Effect of H_2O_2 concentration on *o*-toluidine oxidation; H_2O_2 concentration: 1, 9, 17 and 34 mM with parameter conditions; 1 mM of *o*-toluidine, 1 mM of Fe^{2+}, pH 3 and 100 g of SiO_2

Table 4.8 *O*-toluidine oxidation rates and rate constants at different initial H_2O_2 concentration

H_2O_2 concentration (mM)	Initial rate ($\times 10^{-4}$M min^{-1})	k_h ($\times 10^{-3}$min^{-1})
1	2.61	3.4
9	4.49	21.6
17	5.1	40.4
34	3.5	48.4

In Fe^{2+}/H_2O_2 stage, when H_2O_2 concentration increased from 1 mM to 17 mM, the oxidation rate of *o*-toluidine increased, as shown in Table 4.8. The oxidation rate decreased when H_2O_2 concentration was up to 34. This might be from the scavenging effect of H_2O_2. At the beginning, there was high concentration of H_2O_2. It resulted in more H_2O_2 reacting with ·OH (equation 2.8); therefore, the probability of *o*-toluidine attacked by ·OH was reduced, and the oxidation rate of *o*-toluidine was also reduced (Kahn and Watts, 1996; Moon et al., 1991). In the Fe^{3+}/H_2O_2 stage, the reaction rate increased with the increase of H_2O_2 concentration. When H_2O_2 concentration increased from 1 mM to 34 mM, the pseudo-first-order rate constant increased more than ten times, as shown in Table 4.8.

When H_2O_2 concentration was only 1 mM, there was not enough H_2O_2 to react with Fe^{2+}. From Figure 4.13 (b) and (c), it can be seen that Fe^{2+} remaining for the condition of H_2O_2 1 mM were higher than that of the others, and most H_2O_2 was used in the first stage of reactions. For H_2O_2 9 mM, the regeneration of Fe^{2+} was found after 90 minutes. It is proved by the increase of Fe^{2+} and the decrease of H_2O_2 after 90 minutes. The Fe^{2+} regeneration was not found in 17 and 34 mM of H_2O_2. For the total iron, the least total iron removal can be found in 34 mM of H_2O_2 concentration. This might be from the regeneration of Fe^{2+} from Fe^{3+}, so less Fe^{3+} could be removed by crystallization.

Further analysis on pseudo-first-order rate constant (k_h) showed a linear relationship with respect to H_2O_2 concentration as shown in Figure 4.14. With the equation obtained from the relationship, the k_h in terms of H_2O_2 concentration can be expressed by:

$$k_h = 0.837[H_2O_2]^{0.79} \qquad (4.4)$$

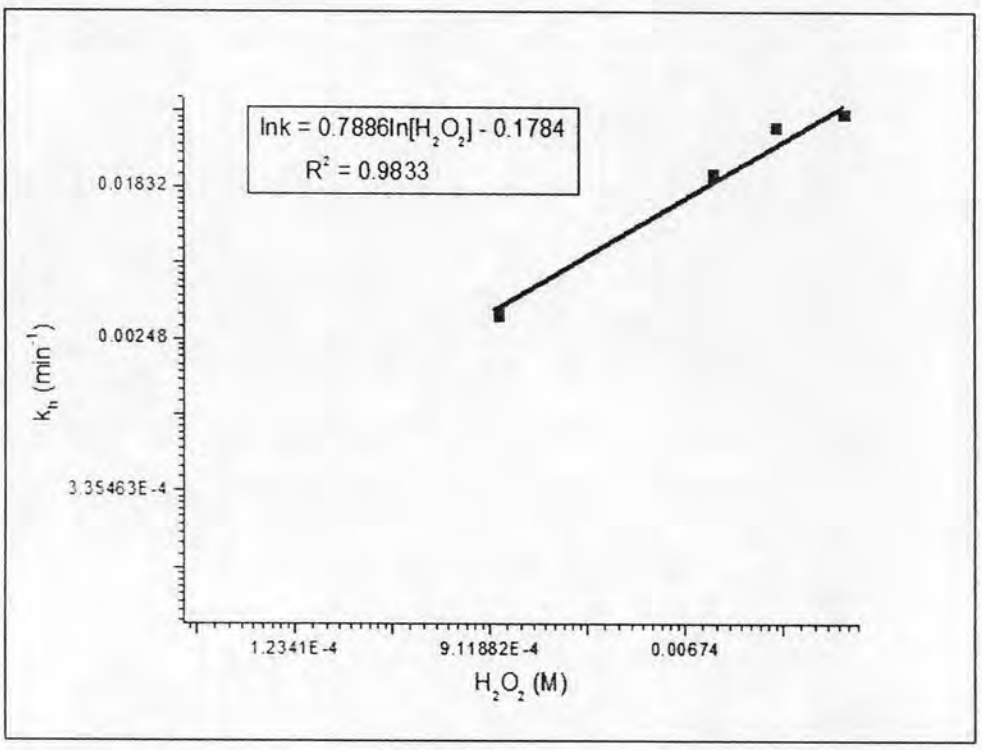

Figure 4.14 Relationship between pseudo-first-order rate constant and initial H_2O_2 concentration; initial condition were as follows: 1 mM of *o*-toluidine, 1 mM of Fe^{2+}, pH 3 and 100 g of SiO_2

4.4.5 Determination of Bi-factor Rate Constant

After the reaction orders with respect to Fe^{2+} and H_2O_2 were known, the reaction rate constant for the Fe^{3+}/H_2O_2 stage (k_{obs}) can be found by combining equations 4.3 and 4.4 as follows:

$$k_{obs} = k[Fe^{2+}]^{1.77}[H_2O_2]^{0.79} \quad (4.5)$$

where k is the bi-factor rate constant.

From non-linear regression between the observed and calculated values from equation 4.5, the "k" that providing the least sum of error squares could be determined to be 2.14×10^5. Consequently, the relationship of k_{obs}, Fe^{2+}, and H_2O_2 can be written as:

$$k_{obs} = 2.14\times10^5[Fe^{2+}]^{1.77}[H_2O_2]^{0.79} \quad (4.6)$$

The plot between observed and calculated rate constant was shown in Figure 4.15. It can be seen that the regression line was fit with the perfect line, with R^2 equals to 0.9525.

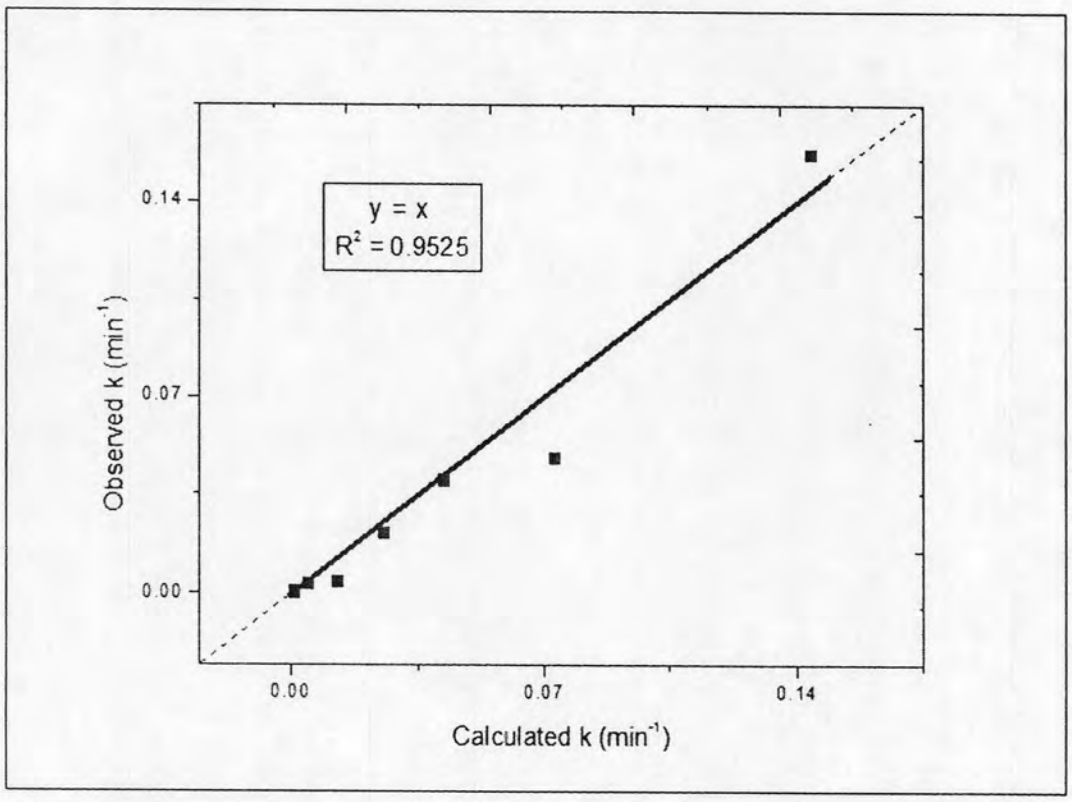

Figure 4.15 Relationship between observed and calculated pseudo-first-order rate constant of *o*-toluidine